MICROSCOPIC CALCULATION OF THE NUCLEONIC LEVELS AND MEAN SQUARE RADII OF ATOMIC NUCLEI WITH THE NEW WOODS–SAXON POTENTIAL PARAMETERS

Z. Łojewski, B. Nerlo-Pomorska

Institute of Physics, Maria Curie-Skłodowska University
Radziszewskiego 10, 20-031 Lublin, Poland

and Jerzy Dudek

Université Louis Pasteur and Institut des Recherches Subatomiques
67037 Strasbourg Cedex 2, France

(Received May 10, 2001; revised version received June 24, 2001)

Single-particle Woods–Saxon Hamiltonian with the new set of parameters adjusted to the experimental single-particle nucleonic levels in spherical nuclei is used to evaluate the mean-square charge radii of even–even, odd–even and even–odd (spherical or deformed) nuclei. The results are compared with the experimental data and with the theoretical values obtained using the single-particle Nilsson potential in the realization of T. Seo. The odd–even staggering of nuclear charge radii is presented and shown to be satisfactorily reproduced by the calculations with the new parametrization.

PACS numbers: 21.10.–k, 21.60.–n

1. Introduction

The use of laser and mass spectroscopy techniques in measurements of the isotopic shifts in the nuclear Mean-Square Charge Radii (MSCR) has resulted in new information concerning this fundamental nuclear property [1-7].

The systematic analysis of the MSCR dependence on the Z and N numbers and, in particular, of the odd–even staggering effects together with that of the nuclear quadrupole moments can be used to test the quality of the underlying theoretical background. A comparison of the corresponding experimental and theoretical results gives a precise information about the spherical and deformed shell closures, the influence of pairing, and important details related to the shape evolution with the nucleon numbers.

Over the years a number of theoretical papers has been devoted to the calculations of the MSCR of even–even as well as odd–A nuclei and there exist several theoretical methods used in the calculations. Examples are provided by the selfconsistent Hartree–Fock or Hartree–Fock–Bogoliubov [8,9] or the Relativistic Mean Field (RMF) calculations [10,11]. These methods, although successful, are relatively computer-time consuming.

The methods based on phenomenological mean single-particle potentials and microscopic–macroscopic approach [12–15] have also been applied in the past; they may serve as a quick and efficient tool to analyze the discussed properties in many nuclear regions.

The aim of the present investigation is to analyze simultaneously the properties of the single-particle nucleonic levels together with those of the mean-square radii of both the even–even and the odd–A nuclei by using the Woods–Saxon (W–S) potential (for the method of solution of the corresponding Schrödinger equation *cf.* Ref. [16]). An axially-symmetric W–S potential with the universal set of parameters [16] has been already applied to calculate the MSCR of the even–even nuclei [15].

In the latter reference it has been shown that it was impossible to reproduce satisfactorily the experimental systematics of the MSCR using the universal parametrization of the W–S mean field. Consequently, it is of interest to find an improved set of parameters which describe simultaneously the shell structure and related microscopic features such as the nuclear MSCR [17]. Indeed, it will be demonstrated in Sect. 3, that a parametrization of the mean-field in question exists offering at the same time an improved description of the single-particle levels and a correct description of the MSCR and of their staggering.

The odd–even staggering of nuclear charge radii is a mechanism that manifests itself through an alternative increasing and decreasing of the MSCR for a fixed Z, when N increases by one unit (*cf. e.g.* [18]). The amplitude of such a variation and possible changes in phase are remarkable manifestations of the occupation of various nucleonic orbitals with increasing N. Within the mean-field approaches the odd–even staggering is explained frequently as a particular manifestation of pairing [19,20] while, when going beyond the mean field concepts, some authors evoke a three- and four-body correlation mechanisms [21,22], or other methods [23]. In the present paper we are going to show that it is possible to reproduce the main features of the odd–even staggering of nuclear charge radii within the framework of a Woods–Saxon mean-field plus the standard BCS [24] approach.

2. The method

The deformed Woods–Saxon potential has been broadly discussed in the literature (*cf. e.g.* Ref. [16] and references therein) and we restrict ourselves to recalling only the basic definitions. The potential consists of the central part $V_{\rm cent}$, the spin–orbit part $V_{\rm so}$ and, for the protons, the Coulomb part $V_{\rm Coul}$:

$$V^{\rm WS}(\vec{r},\vec{p},\vec{s};\beta) = V_{\rm cent}(\vec{r};\beta) + V_{\rm so}(\vec{r},\vec{p},\vec{s};\beta) + V_{\rm Coul}(\vec{r};\beta) \tag{1}$$

with[1]

$$V_{\rm so}(\vec{r},\vec{p},\vec{s};\beta) = -\lambda(\nabla V_{\rm cent} \wedge \vec{p})\cdot\vec{s}. \tag{2}$$

The central potential is defined by:

$$V_{\rm cent}(\vec{r};\beta) = \frac{V_0[1 \pm \kappa(\frac{N-Z}{N+Z})]}{\{1+\exp[{\rm dist}_\Sigma(\vec{r};\beta)/a]\}}, \tag{3}$$

where a characterizes the diffuseness of the nuclear surface. The function ${\rm dist}_\Sigma(\vec{r},\beta)$, describing the distance between a given point $\vec{r}$ and the nuclear surface is determined numerically [16]. In the above formulae β stands for the ensemble of parameters $\{\beta_\lambda;\lambda=2,4,...\}$ characterizing the nuclear shape:

$$R(\theta;\beta) = c(\beta)R_0\left[1+\sum_\lambda \beta_\lambda Y_{\lambda 0}(\cos(\theta)\right], \tag{4}$$

where $R_0 = r_0 A^{1/3}$. Function $c(\beta)$ insures the nuclear volume conservation when surface Σ is being deformed.

The charge mean square radii are calculated using the expression

$$\langle r^2\rangle_{\rm even} = \sum_{\nu>0} 2\langle\nu|r^2|\nu\rangle v_\nu^2 + 0.64\,{\rm fm}^2 \tag{5}$$

for even Z systems, and as

$$\langle r^2\rangle_{\rm odd} = \sum_{\substack{\nu\neq\nu_1\\ \nu>0}} 2\langle\nu|r^2|\nu\rangle v_\nu^2 \;+\; \langle\nu_1|r^2|\nu_1\rangle \;+\; 0.64\,{\rm fm}^2 \tag{6}$$

for the odd ones. Proton single-particle wave-functions corresponding to paired levels are denoted by $|\,\nu\rangle$ while $|\,\nu_1\rangle$ denotes a wave-function of an unpaired particle. Term 0.64 fm^2 originates from the finite-size distribution of the proton charge [25]. The single-particle occupation factors v_ν are calculated within the standard BCS formalism with the blocking procedure applied for odd–A systems.

[1] Strictly speaking, the mathematical form of the function acted upon with the gradient in Eq. (2) is identical with that of the central potential, but the numerical values of the geometrical parameters used are different from those of the central part as indicated below.

3. Adjustment of parameters

Generally, to define the W–S Hamiltonian 12 constants (6 for protons and 6 for neutrons) must be determined. One can divide these parameters into two groups. The first one is composed of parameters that describe the central part of the W–S potential:

V_0 — the depth parameter of the central potential,

r_0 — the corresponding radius parameter, and

a_0 — the diffuseness parameter.

The second one is composed of parameters that describe the spin–orbit term:

λ — the strength parameter of the spin–orbit potential,

$r_{\rm so}$ — the corresponding radius parameter, and

$a_{\rm so}$ — the diffuseness parameter.

The parameters of the first group above influence first of all the single-nucleon binding energies and the global nuclear features such as the mean square radii, and, at a fixed deformation, the quadrupole moments. The parameters of the second group influence first of all the order and the relative distances among the single particle levels.

Several sets of the W–S parameters have been proposed in the literature (see *e.g.* Ref. [16] and references therein). All the parameters were fitted to the contemporarily existing experimental single-particle levels of (mostly) spherical nuclei [26].

The 'universal' set of parameters has been obtained by adopting the parametrization of the central potential from Rost, Ref. [27], and adjusting the spin–orbit potential parameters from the order of the experimentally known band-head properties of the *deformed* nuclei. No attention has been paid at that time to the reproduction of the MSCR and it was demonstrated later on in Ref. [28] that the proton radius of the 'universal' parametrization should be reduced by $\sim 2\%$ in order to reproduce systematically the calculated $B(\mathrm{E2})$ values (*cf.* Ref. [29]). This deficiency of the 'universal' parametrization results in too high values of the MSCR as illustrated in Fig. 1, where the mean square charge radii of rare-earth isotopes obtained with the 'universal' parameters of the W–S Hamiltonian are compared with those of the Nilsson Hamiltonian [30] as well as with the experimental data [1]. One could have thought at first that a simple modification of the proton radius parameter would have been sufficient to remedy this deficiency. However calculations show that the quality of the description of the

single-particle energies deteriorates when trying such a simple manipulation and a physically correct solution of the problem is to refit all the parameters. This is particularly worth doing given a much richer experimental data basis as compared to that of the original early studies dating 30 to 40 years back.

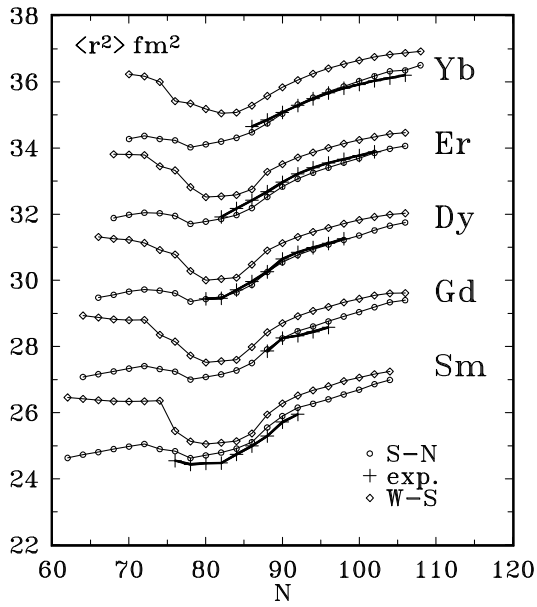

Fig. 1. Experimental MSCR, in fm^2, (from Ref. [1], crosses) of Sm–Yb nuclei taken as an example as functions of the neutron number, compared to calculation results obtained with the W–S potential with 'universal' parametrization (empty diamonds) and corresponding results obtained by using the Nilsson Hamiltonian of Seo Ref. [29], open circles. The left-hand side scale corresponds to Samarium elements. For clarity the results of the remaining nuclei are shifted upwards by 2, 4, ... fm^2.

In the present work we have refitted the parameters of the Woods–Saxon Hamiltonian by adjusting them to the experimental results on the single-particle energy levels of doubly-magic nuclei, mean square radii $\langle r^2 \rangle$ (for neutrons and protons), and neutron, S_n, and proton, S_p, separation energies. The most important criterion for a choice of the best parameters of the W–S potential is of course the agreement between the theoretical and experimental single-particle energy levels. We have restricted our analysis of the single-particle levels to those known from the doubly magic nuclei ^{40}Ca, ^{48}Ca, ^{56}Ni, ^{90}Zr, ^{132}Sn, ^{208}Pb. Next, however, we have verified that the deformation dependence of the single-particle energy levels is well gen-

erated by the W–S potential and consequently a good agreement also for the positions of the band-heads of the deformed odd–A nuclei, by using the same Hamiltonian, has been obtained.

The coupling of the single-particle orbitals to the collective-vibrations has been neglected here. Estimates based, among others, on the RPA treatment indicate (*cf.* Refs. [31] and [32]) that possible shifts due to the vibration-coupling are typically of the order of 200 keV (being sometimes positive and sometimes negative) and seldom exceed 300 keV — thus having only a rather insignificant influence on our adjustment procedure.

As mentioned above, the second group of important observables to take into account are the proton and neutron mean square radii. In the literature there exists a rich collection of the experimental values of proton square radii $\langle r_p^2 \rangle$ [1,2,5]. In this work we have used them to optimize the central part of the proton W–S potential. The experimental neutron radii, $\langle r_n^2 \rangle$, can be deduced from the analysis of the high-energy polarized proton scattering [34] and from the $\pi^{\pm}$ scattering [33]. The values of neutron radii are usually given with large error. However, they provide a precious tool for definition of the correct size of the central part of the neutron W-S potential. The neutron, S_n, and proton, S_p, separation energies serve as an auxiliary criterion permitting to obtain the correct depths of the potentials.

As a measure of the fit error the root-mean-square deviation σ has been chosen, defined as usual by:

$$\sigma = \left[\frac{1}{n-1} \sum_{i=1}^{n} \left(f_{\mathrm{exp}}^{(i)} - f_{\mathrm{th}}^{(i)} \right)^2 \right]^{1/2} . \tag{7}$$

Here $f_{\mathrm{th}}^{(i)}$ are the calculated, and $f_{\mathrm{exp}}^{(i)}$, the corresponding measured quantities. The number of the experimental data points is n. The experimental single-particle energies form a part of ensemble $\{f_{\mathrm{exp}}^{(i)}\}$ together with the separation energies and MSCR, leading to three types of deviations, σ_e, σ_s and σ_r, respectively. It turns out that a more convenient expression to be minimized is:

$$\sigma = w_e \cdot \sigma_e + w_S \cdot \sigma_S + w_r \cdot \sigma_r , \tag{8}$$

where three weight factors w_e, w_s, and w_r are the theoretical weights corresponding to the various observables ($w_i \sim 1/\sigma_i$) where σ is the "theoretical average" error for i-observable. We used the following weight factors: $w_e = 1.0\,[1/\mathrm{MeV}]$, $w_s = 1.6\,[1/\mathrm{MeV}]$ and $w_r = 10.0\,[1/\mathrm{fm}]$. We accept the fit of the W–S potential parameters if they reproduce the experimental $\langle r^2 \rangle$ within the experimental accuracy (or at least to be a very close). Such a condition is equivalent to imposing a very high weight factor w_r in front of σ_r; usually $w_r \sim 5$ to 10 is a sufficient choice.

For the single particle energies the calculations have been performed for the above mentioned six double-magic nuclei. This determines, on the whole, 31 known $(2j+1)$-degenerate levels for protons and 48 $(2j+1)$-degenerate levels for neutrons.

The best set of the W–S parameters has been found by minimizing the standard deviations introduced above in the space of six parameters (V_0, r_0, a_0, λ, $r_{\rm so}$ and $a_{\rm so}$) for protons and neutrons each. We have used as the starting values the ones corresponding to the 'universal' set of parameters allowing for the variations in the following ranges: $V_0 \in (46 \div 55)$ MeV, $r_0 \in (1.10 \div 1.40)$ fm, $a_0 \in (0.50 \div 0.80)$ fm, $\lambda \in (10 \div 80)$, $r_{\rm so} \in (1.10 \div 1.40)$ fm and $a_{\rm so} \in (0.50 \div 0.80)$ fm.

The resulting best fit parameters obtained here and the 'universal' ones, used as a reference, are compared in Table I. While the potential depth parameters do not differ very much, the isospin dependence of the central potential well is found nearly 20% weaker in the new parametrization — the result based on a much larger experimental information as compared to that known when the 'universal' set was established. The coupling constants of the spin–orbit potentials are found now markedly lower, compared to the corresponding parameters of the 'universal' set. Also the corresponding values of the spin–orbit radius parameters are significantly lower. In order to understand better this aspect of the new fit we have analyzed in more detail the behavior of σ_e of Eqs. (7),(8). For this purpose we have tabulated σ_e in function of $r_{\rm so}$ and λ, all other parameters fixed as in Table I, for neutrons and protons separately.

TABLE I

Comparison of the W–S potential parameters: the 'universal' ones treated as a reference are given in column 3, and the 'best fit' of the present work, given in column 4. Parameter values for $r_{\rm so}$ and λ correspond to the minima of functions σ_e in Figs. 2 and 3. For apparent differences in the λ-values for protons and neutrons see text.

Parameter	Units	Univ.	Present
V_0	MeV	49.600	51.500
κ	—	0.860	0.650
a_0^n	fm	0.700	0.610
r_0^n	fm	1.347	1.263
λ_n	—	35.000	24.000
$r_{\rm so}^n$	fm	1.310	1.140
a_0^p	fm	0.700	0.610
r_0^p	fm	1.275	1.258
λ_p	—	36.000	18.000
$r_{\rm so}^p$	fm	1.320	1.140

The results are illustrated in figures 2 and 3, respectively. As it is seen from the figures, in the discussed parameter range the optimal spin–orbit radius parameters vary nearly linearly with the spin–orbit strengths, the corresponding behavior of σ_e having a form of a valley.

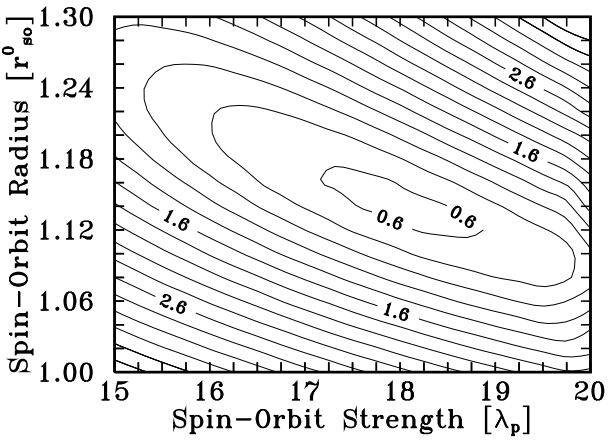

Fig. 2. The root-mean-square deviation σ_{e_p} for protons as the function of the spin–orbit strength λ_p and spin–orbit radius $r^p_{\rm so}$ parameters of the Woods–Saxon potential. This result has been obtained in two steps. Firstly, it has been checked that the results for σ_e for the nuclei studied have similar behavior as functions of $r^p_{\rm so}$ and λ_p and that minima for all the nuclei lie close one to another in the $(r_{\rm so}, \sigma)$ plane. Secondly, σ_e corresponding to all the nuclei has been obtained by summing up the contributions σ_e from the individual nuclei.

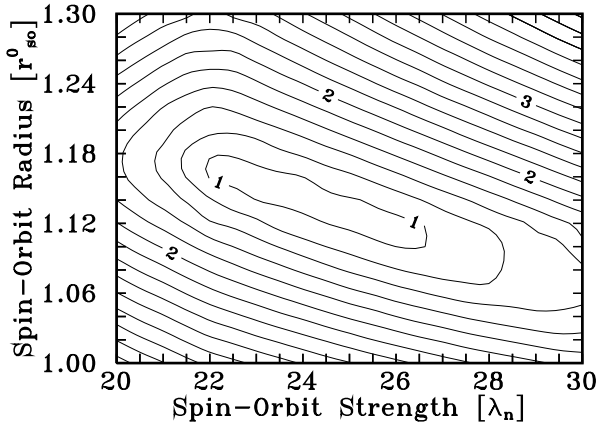

Fig. 3. The same as in Fig. 2 for neutrons.

It can be expected, from an approximate isospin invariance of nuclear forces, that the proton and neutron strength parameters of the spin–orbit interactions have very close values. As it is seen in Table I, these values taken from Figs. 2 and 3 as the minima of σ_e functions are λ_p=18 and λ_n=24, for protons and neutrons, respectively. This relatively big difference of about 25% may be viewed as only apparent. Indeed, because of a flat dependence of σ_e on $r_{\rm so}$ and λ along the valleys an alternative choice of $\lambda_n \sim \lambda_p$ and $r^n_{\rm so} \sim r^p_{\rm so}$ is possible. In the vicinity of the local minima found and without loosing much in terms of quality of the fit (the latter measured in terms of σ_e) we can use the following two linear approximations for the $r_{\rm so}$ *vs.* λ relations:

$$\text{Protons}: r^p_{\rm so} = \alpha_p \lambda_p + \beta_p; \quad \alpha_p = -0.0345, \quad \beta_p = 1.769 \tag{9}$$

and

$$\text{Neutrons}: r^n_{\rm so} = \alpha_n \lambda_n + \beta_n; \quad \alpha_n = -0.0140, \quad \beta_n = 1.487. \tag{10}$$

The root-mean-square errors $\sigma_{\langle r_{ch}\rangle}$ obtained for all nuclei with the experimental values taken from Ref. [2], and those for the neutrons, $\sigma_{\langle r_n\rangle}$, experiment from Ref. [34], together with the binding energy deviations, σ_{S_p} and σ_{S_n} (experiment from [35]) are presented in Table II. Comparison shows that the new parametrization offers an important improvement over the 'universal' set for all the four quantities analyzed, while the energy level deviations σ_{e_n} and σ_{e_p} remain comparable for the two sets of parameters.

TABLE II

Comparison of the fit quality in terms of the standard deviations. In the table we take into account 142 nuclei when calculating $\sigma_{\langle r_{ch}\rangle}$ [5], 14 nuclei for $\sigma_{\langle r_n\rangle}$ [33, 34] and correspondingly 332 and 341 nuclei for σ_{S_n} and σ_{S_p} [37]. Values σ_{e_n} and σ_{e_p} are given for above mentioned six double-magic nuclei.

	$\sigma_{\langle r_{ch}\rangle}$ fm	$\sigma_{\langle r_n\rangle}$ fm	σ_{S_n} MeV	σ_{S_p} MeV	σ_{e_n} MeV	σ_{e_p} MeV
New	0.026	0.091	0.411	0.385	0.90	0.54
Univ.	0.082	0.247	0.530	0.740	0.88	0.76

The proton and neutron single-particle levels for the doubly-magic nuclei studied are illustrated in figures 4–9. One can see that the 'best fit' parameters give slightly, but systematically better agreement with the experiment.

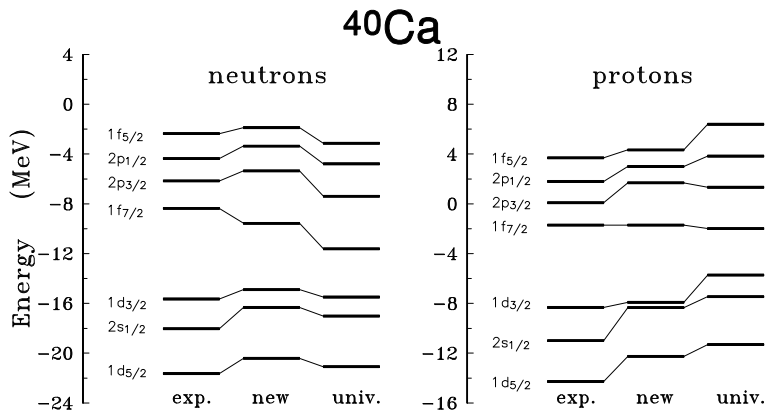

Fig. 4. Single-particle energy levels for ^{40}Ca nucleus: left — neutrons, right — protons.

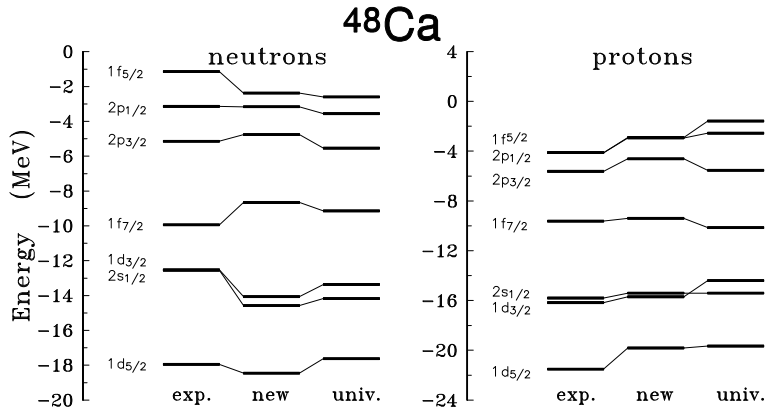

Fig. 5. Single-particle energy levels for ^{48}Ca nucleus: left — neutrons, right — protons.

The new set of parameters introduced in this work reproduces particularly well the single-particle proton levels. For all double-magic nuclei the order of levels is correct. Also σ_{S_p}-deviation is comparatively small (σ_{e_p}=0.54) see Table II. The results are slightly worse for the neutrons. Here σ_{e_n}-deviation is not better than for universal parametrization (σ_{e_n}=0.90) but also in this case the order of the single-particle energy levels is good.

The quality of comparison between the single-particle energy spectra with the 'universal' parametrization and experiment can be considered very good — even though slight improvements were possible. It should, however, be emphasized that the non-linear problem studied here allows for the existence of rather numerous local minima of the σ-test in the space of

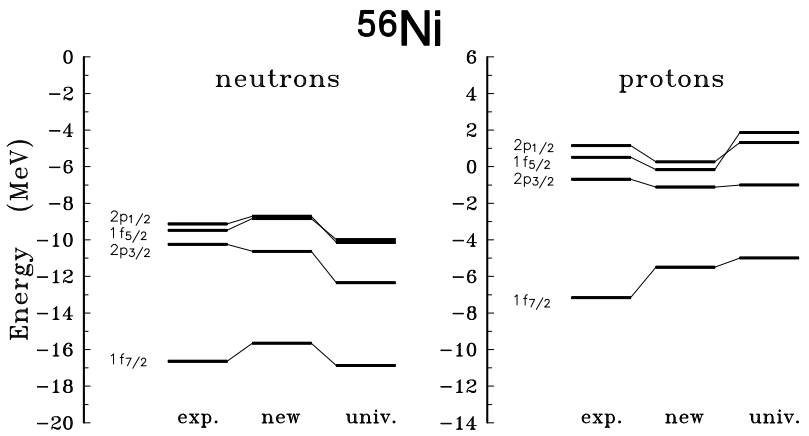

Fig. 6. Single-particle energy levels for ^{56}Ni nucleus: left — neutrons, right — protons.

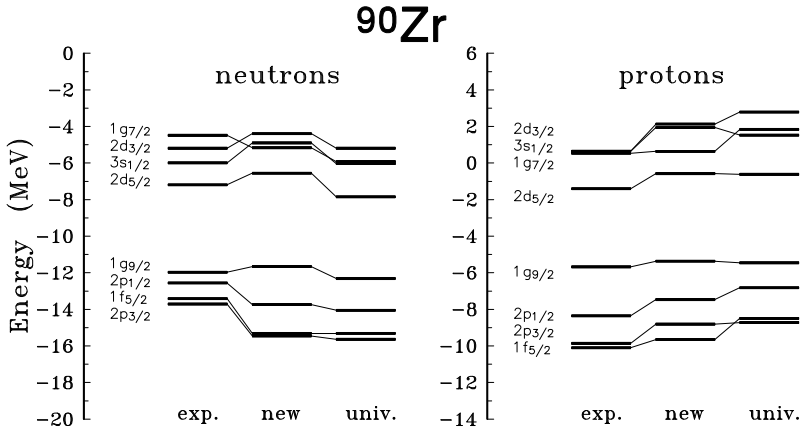

Fig. 7. Single-particle energy levels for ^{90}Zr nucleus: left — neutrons, right — protons.

the six variables studied. By imposing the condition that the experimental mean-square radii be reproduced we must eliminate some of the mentioned minima as 'unphysical' — yet there are usually a few local minima left that reproduce the single-particle energy spectra quite well.

Our fitting procedure suggests that it will be most likely impossible to improve the quality of description of the experimental results without modification of the formalism *e.g.* by introducing the potentials more complex than the Woods–Saxon and for taking into account the coupling with the collective degrees of freedom.

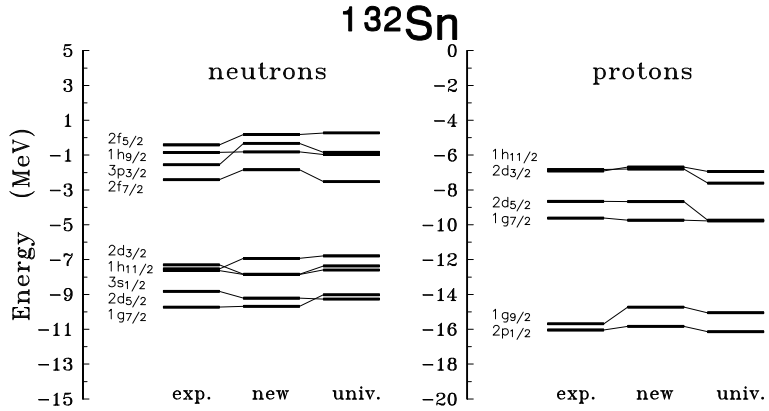

Fig. 8. Single-particle energy levels for ^{132}Sn nucleus: left — neutrons, right — protons.

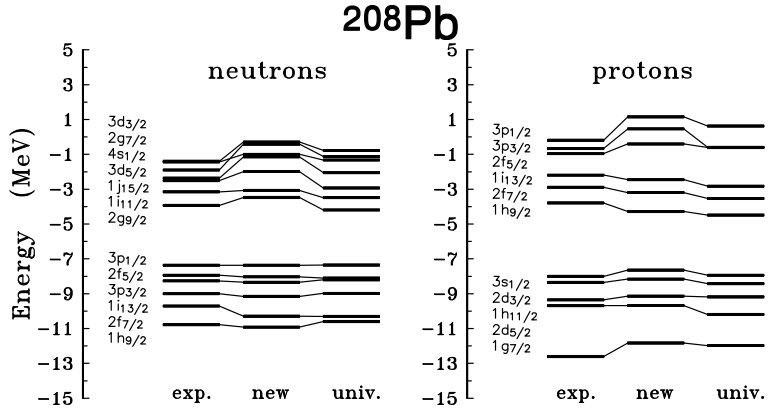

Fig. 9. Single-particle energy levels for ^{208}Pb nucleus: left — neutrons, right — protons.

4. Charge mean square radii

The charge mean square radii have been calculated at the equilibrium deformations taken from Ref. [36]. The pairing interaction has been included by the BCS approximation using the experimental energy gaps [35], obtained from three-point mass formula. For the odd–A nuclei, the odd particle has been placed in the state nearest to the Fermi level for which the angular momentum projection Ω and parity π are the same as the experimental ones. When the experimental data were not known, we have placed the odd–particle in the state nearest to- but higher than- the Fermi level.

The calculations were performed for nuclei with $37 < Z < 54$ and $Z < N < 78$, for the rare earth nuclei with $55 < Z < 79$ and $74 < N < 120$ and for the actinides with $80 < Z < 94$ and $101 < N < 150$. In the present work we show only the results for the experimentally known nuclei and their close neighbors *i.e.* the nuclei for which we may hope to know the experimental results in near future. The quality of the fit can be judged through a systematic comparison of the dependence of the neighboring isotopes on a neutron number N.

In Figs. 10–14 the MSCR of the investigated elements are presented for a fixed $Z-$ and variable $N-$numbers. Theoretical values, obtained with the help of the WS+BCS approach are represented by open circles, while the experimental data of Ref. [1] by crosses. The curves are labeled by the chemical symbols of the elements. The left-hand side scale corresponds to the lightest element. All other curves are shifted upwards by 2, 4, ... fm^2 for clarity of the illustration.

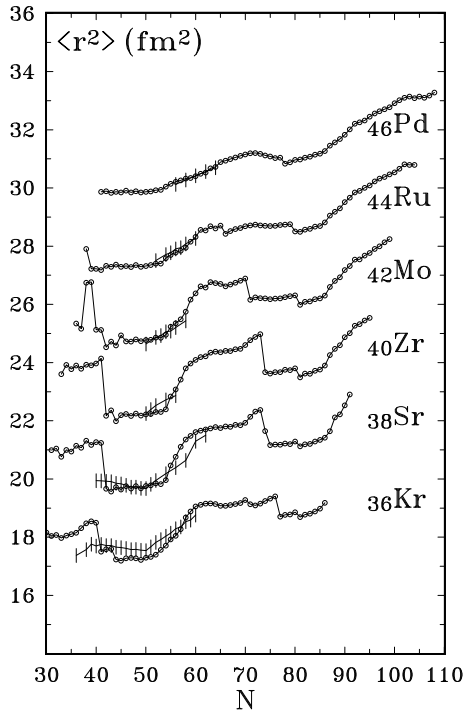

Fig. 10. Charge mean square radii of Kr–Pd nuclei, in fm^2, as functions of the neutron number. Crosses denote the experimental data from Ref. [1], the open circles the theoretical results obtained with the Woods–Saxon single particle potential, parameters of this work. The left-hand side scale corresponds to the krypton nuclei. For clarity the results of the remaining nuclei are shifted upwards by 2, 4, ... fm^2.

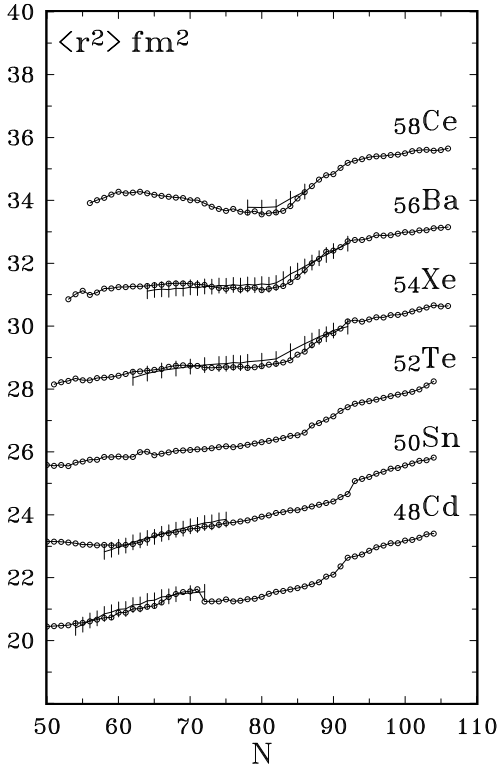

Fig. 11. The same as in Fig. 10 but for Cd–Ce nuclei.

In Fig. 10 the MSCR of even elements Kr–Pd are shown. One can see a marked increase in the radii for $N \sim 50$-60 in several elements, also clearly present in the experimental data. An abrupt change in the radii in the vicinity of $N = 42$ is not confirmed by the data on krypton, although a change in structure at N=40 is confirmed together with the corresponding slope. The predictions of sharp irregularities at $N \sim 40$ and $N \sim 72$ can be related to the shape coexistence (in particular: prolate *vs.* oblate shape coexistence for the first of the two) whose precise description is sometimes less certain. They are related to the uncertainties in the calculations of the *equilibrium deformations* which are known to be a bit more difficult for 'transitional' nuclei whose Z and/or N numbers are close to those of the strong magic shell closures.

The kink of MSCR values when crossing the $N = 50$ magic number would probably be better reproduced through the inclusion of the quadrupole pairing forces [38].

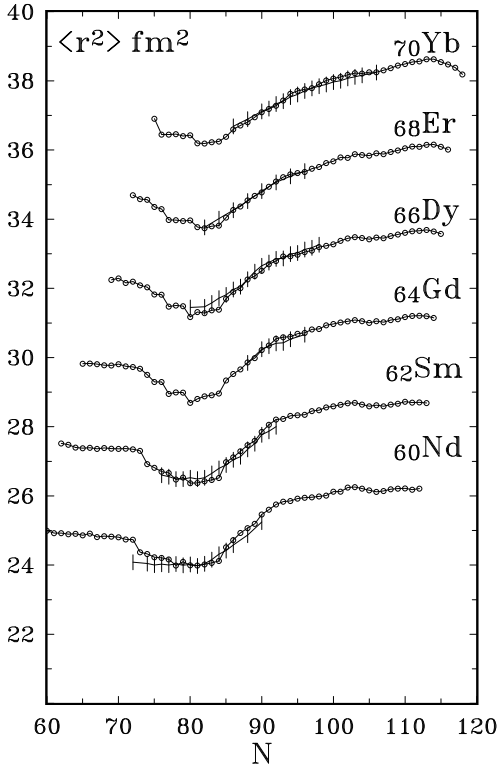

Fig. 12. The same as in Fig. 10 but for Nd–Yb nuclei.

The agreement of MSCR with experimental data improves for the stronger-deformed Cd–Ce nuclei. A series of results for even–even elements of this group is presented in Fig. 11. Only a small irregularity in MSCR for $N = 72$ is obtained in the calculations, so far not seen in experiment.

The next MSCR, for Nd–Yb elements shown in Fig. 12, agree also well with the experimental data. The characteristic dependence of the MSCR on the neutron number in Nd, Sm and Dy nuclei when crossing the $N = 82$ magic number is well reproduced.

Similar relations are also true in the case of the MSCR of odd-Z elements, Pr–Lu, shown in Fig. 13. Since the characteristic behavior of results for Eu isotopes around N=82 is well verified by experiment one may expect that similarly the predictions for $_{59}$Pr, $_{61}$Pm and $_{65}$Tb will be confirmed. Although the theoretical results for Lu are slightly smaller and for Tm larger than the experimental ones, they have the correct N dependence.

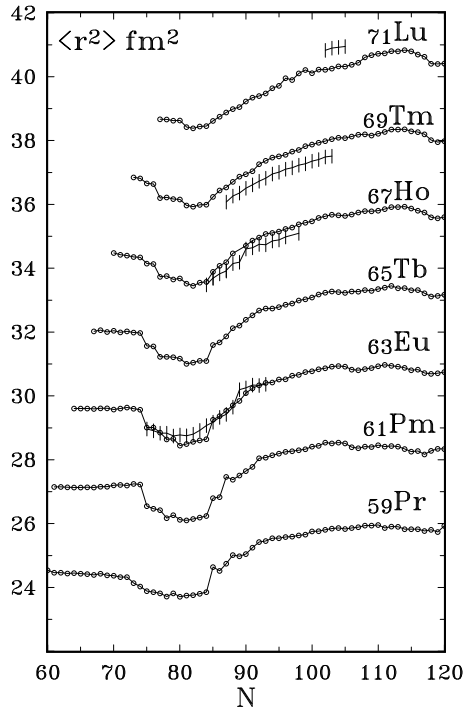

Fig. 13. The same as in Fig. 10 but for Pr–Lu nuclei.

The results for the heaviest Au–Ra nuclei are presented in Fig. 14. Their MSCR show already some irregularities in experimental data. A strong staggering in the lightest Hg isotopes is not reproduced, though predicted for the light Fr and Ra nuclei. The ^{193}Pb, ^{224}Rn and ^{225}Rn MSCR values of Ref. [1] seem off the trend manifested by all the other nuclei in the neighborhood and are not reproduced by our calculation. The predictions for some of the Ra and Th elements have to be taken with some caution, because the octupole deformation can be present there and influence the MSCR values. The octupole degrees of freedom were not taken into account when calculating the equilibrium deformations in this work.

The general tendencies in the dependence of the MSCR values on the neutron number are well reproduced by our WS+BCS approach. In some cases a more detailed discussion of the structure effects is needed in order to explain subtle discrepancies which still exist. Figures 10–14 demonstrate in particular that the slopes of the illustrated curves in terms of N are correct. A good agreement of MSCR in most cases confirms a very satisfactory quality of the new Woods–Saxon potential parameters.

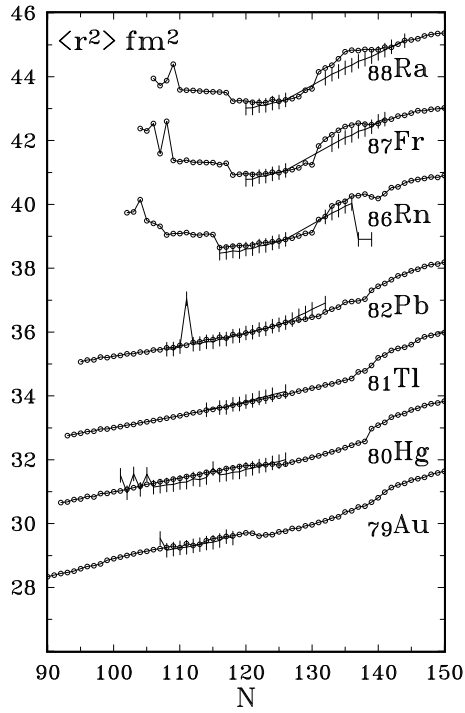

Fig. 14. The same as in Fig. 10 but for Au–Ra nuclei.

5. Odd–even staggering effect in MSCR

A detailed analysis of the MSCR experimental data shows regular deviations between the odd- and the even-isotopes for several elements. Usually, when going from an odd to an even system, the radius grows slower than when going from an even to an odd one. In order to describe those differences quantitatively a differential isotopic MSCR shift can be introduced:

$$\delta\langle r^2\rangle^{A,A-1} = \langle r^2\rangle^{A} - \langle r^2\rangle^{A-1}. \tag{11}$$

Within the mean field theories the discussed effects can be attributed to the role of the pairing correlations that capture the next nucleon onto the so far unpaired level thus contributing to a decrease in the deformation of the charge density distributions for even particle number. As one can see in formulas (6) a radius of odd Z system depends not only on the equilibrium deformation of a whole Z, N nucleus, which influences the single particle level scheme and the BCS equations solution, but also on the state $|\nu_1\rangle$ occupied by the odd proton.

It should be possible — close to the Fermi surface, to minimize the total potential energy and correspond to the experimentally known spin of the nucleus (Z, N). These three conditions are sometimes difficult to achieve because very often the most probable quasiparticle α_{ν_1} should be created in the ν_1 state lying under the Fermi surface in order to reproduce the proper spin of this nucleus. The order of single particle levels close around the Fermi surface is very important for the proper reproduction of odd–even staggering of nuclear radii, but its impossible to take this subtle effect into account during the W–S parameters fit not loosing the larger effects in the whole single particles levels schemes, binding energies and even–even nuclei radii.

It is generally difficult to obtain a quantitative agreement between the very tiny (only 0.03%) odd–even experimental staggering in MSCR and a simple macroscopic–microscopic description because the parameters of the single particle potential, those of the macroscopic term and the pairing strengths influence the whole potential energy surface. A realistic, deformation-dependent single particle level scheme is crucial for the description of the odd-particle states. It turns out that our new parametrization of the mean field gives very satisfactory results in this respect. Although there are some remaining discrepancies they are smaller in the case of the new Woods–Saxon as compared to the Nilsson model of Seo [30] as it is illustrated below.

As an illustration of our calculations, the differential isotopic MSCR shifts $\delta\langle r^2\rangle^{A,A-1}$ are shown for the Cd (even Z) and for the Ho (odd Z) nuclei in Fig. 15. The MSCR differential isotopic shifts obtained with the Woods–Saxon single particle potential are marked by open circles and with Seo–Nilsson [30] by open squares.

For Cd isotopes shown in the figure the agreement of both models with experimental data is satisfactory for $N \sim 60$ and slightly worse for $N \sim 50$ and $N \sim 70$ nuclei. The W–S potential gives smaller odd–even staggering as compared to the Seo–Nilsson model in most of the cases in better agreement with experiment. In the discussed nuclei the average staggering effect has a proper sign, but it is exaggerated in some cases.

In Fig. 16 the odd-Z Ho nuclei are shown. The theoretical values of the staggering are too large in comparison with the experimental data, but the qualitative behavior is reproduced. For odd–odd nuclei the coupling of the two odd nucleons exists. Investigations of such a coupling are in progress now.

The best agreement is achieved for Pb isotopes (Fig. 17) where the experimental odd–even staggering is reproduced. For the magic number $Z = 82$ the parameters of all the theoretical models are well established so, on the one hand, the results fitted to the experimental data could be expected to agree well. On the other hand it is also likely that in the presence of the strongest shell closures the coupling to the collective degrees of freedom (neglected here) is the weakest.

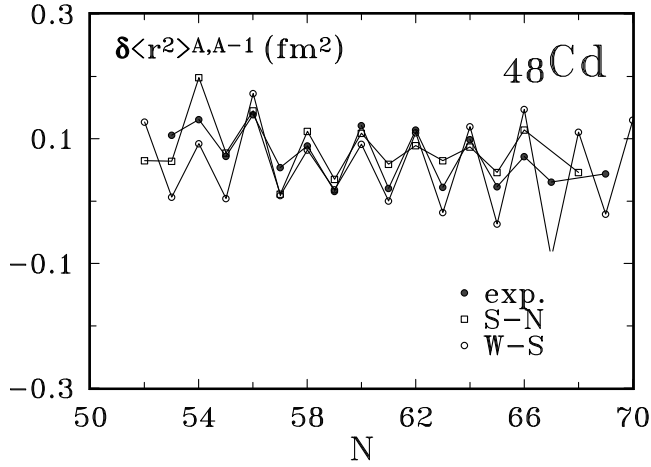

Fig. 15. The differential shifts $\delta\langle r^2\rangle^{A,A-1}$ of the charge mean square radii, in fm^2, for Cd isotopes as functions of the neutron number. The dots denote the experimental data from Ref. [2], open circles the theoretical results obtained with the Woods–Saxon single particle potential with parameters of this work, the squares with the Seo–Nilsson one [30].

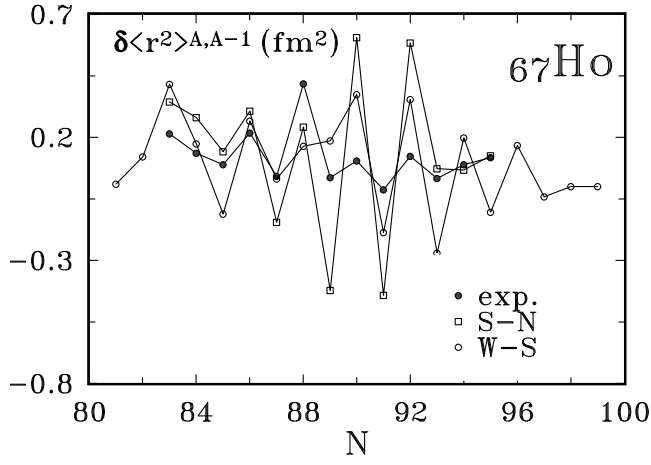

Fig. 16. The same as in Fig. 15 but for Ho isotopes.

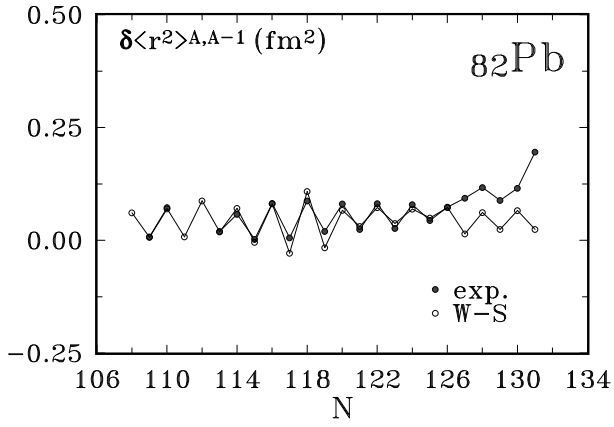

Fig. 17. The same as in Fig. 15 but for Pb isotopes.

6. Summary and conclusions

In this article we have studied the properties of the nuclear deformed mean field parametrized in terms of the Woods–Saxon potential. By using the experimental data on the single-particle levels in the doubly-magic spherical nuclei, on the r.m.s radii in the nuclei for which they are known and on the separation energies in the deformed nuclei we have found a new set of the Woods–Saxon potential parameters that offers a better description in terms of these observables.

We have applied the macroscopic–microscopic method with the obtained here Woods–Saxon single-particle potential parameters in order to calculate the MSCR and the odd–even staggering effects in couple of hundreds nuclei throughout the periodic table. The corresponding results have been counterchecked by using the Seo–Nilsson deformed harmonic oscillator potential known to perform well in the calculations of this type.

The odd–even charge staggering effect has been satisfactorily reproduced in many nuclei studies, although in details disagreements remain. It is worth emphasizing that the neutron dependence in the experimental mean-square-charge-radii has been generally very well reproduced.

The authors would like to thank Prof. K. Pomorski for valuable discussions and comments. Some of us, B.N.-P. and Z. Ł. would like to express their gratitude to the Institut de Recherches Subatomiques and the UFR de Sciences Physiques of the University Louis Pasteur of Strasbourg for hospitality. This research was partially supported by the French–Polish cooperation program POLONIUM and the Polish State Committee for Scientific Research (KBN) grant No. 2P03B11519.

REFERENCES

[1] H. de Vries, C.W. de Jager, C. de Vries, *At. Data Nucl. Data Tables* **36**, 495 (1987).

[2] E.W. Otten; *Treatise on Heavy Ion Science* **Vol. 8**, Ed. by D. Allan Bromley, Plenum Press, New York 1989, p. 517.

[3] P. Aufmuth, K. Heiling, A. Steudel, *At. Data Nucl. Data Tables* **37**, 455 (1985).

[4] S. Raman, C.H. Malarkey, W.T. Milner, C.W. Nestor Jr., P.H. Stelson, *At. Data Nucl. Data Tables* **36**, 1 (1987).

[5] E.G. Nadjakov, K.P. Marinova, *At. Data Nucl. Data Tables* **56**, 133 (1994).

[6] J. Billowes, P. Cambel, *J. Phys. G* **21**, 707 (1995).

[7] G. Fricke, C. Bernhard, K. Heilig, L.A. Schaller, L. Schellenberg, E.B. Shera, C.W. de Jager, *At. Data Nucl. Data Tables* **60**, 177 (1995).

[8] J.W. Negele, D. Vautherin, *Phys. Rev.* **C5**, 1472 (1972).

[9] J. Dobaczewski, W. Nazarewicz, T.R. Werner; *Z. Phys.* **A45**, 27 (1996).

[10] M.M. Sharma, P. Ring, *Phys. Rev.* **C45**, 2514 (1992).

[11] K. Pomorski, P. Ring, G.A. Lalazissis, A. Baran, Z. Łojewski, B. Nerlo-Pomorska, M. Warda, *Nucl. Phys.* **A624**, 349 (1997).

[12] B. Nerlo-Pomorska, K. Pomorski, B. Skorupska-Mach, *Nucl. Phys.* **A562**, 80 (1993).

[13] B. Nerlo-Pomorska, B. Skorupska-Mach, *At. Data Nucl. Data Tables* **60**, 285 (1995).

[14] B. Nerlo-Pomorska, K. Pomorski, J. Puszyk, *Acta Phys. Pol.* **B27**, 537 (1996).

[15] Z. Łojewski, B. Nerlo-Pomorska, K. Pomorski, J. Dudek, *Phys. Rev.* **C51**, 601 (1995).

[16] S. Ćwiok, J. Dudek, W. Nazarewicz, J. Skalski, T. Werner, *Comput. Phys. Commun.* **46**, 379 (1987).

[17] Z. Łojewski, J. Dudek, *Acta Phys. Pol.* **B29**, 407 (1998).

[18] G.D. Alkhazov, A.E. Bazrakh, V.A. Bolshakov, V.P. Denisov, V.S. Ivanov, Yu.Ya. Sergeyev, I.Ya. Chubukov, V.I. Tikhonov, V.S. Letokhov, V.I. Mishin, S.K. Sekatsky, V.I. Fedoseyev, *Z. Phys.* **A337**, 257 (1990).

[19] B.S. Reehal, R.A. Sorensen, *Nucl. Phys.* **A161**, 385 (1971).

[20] M. Horoi, *Phys. Rev.* **C50**, 2834 (1994).

[21] D. Zawischa, U. Regge, R. Stapel, *Phys. Lett.* **185**, 299 (1987).

[22] U. Regge, D. Zawischa, *Phys. Rev. Lett.* **61**, 149 (1988).

[23] S.A. Fayans, S.V. Tolokonnikov, E.L. Trykov, D. Zawischa, *Nucl. Phys.* **A676**, 49 (2000).

[24] J. Bardeen, L.H. Cooper, I.L. Schrieffer, *Phys. Rev.* **106**, 162 (1957).

[25] P. Quentin, *Nuclear Self-Consistent Fields,* eds. G. Ripka, M. Porneuf, North Holland, Amsterdam 1977.

[26] A. Bohr, B.R. Mottelson, *Nuclear Structure*, Vol. 1, W.A. Benjamin Inc., New York, Amsterdam 1969.

[27] E. Rost, *Phys. Lett.* **B26**, 184 (1968).

[28] S. Kahane, S. Raman, J. Dudek, *Phys. Rev.* **C40**, 2282 (1989).

[29] See Sect. V of Ref. [28].

[30] T. Seo; *Z. Phys.* **A324**, 43 (1986).

[31] A. Oros, Ph.-D. Thesis, 1998, University of Köln, unpublished.

[32] M. Rejmund, Ph.-D. Thesis, 1998, University of Warsaw.

[33] W.R. Gibbs, J.P. Dedonder, *Phys. Rev.* **C46**, 1825 (1992).

[34] C.J. Batty, E. Friedman, H.J. Gils, H. Rebel, *Adv. Nucl. Phys.* **19**, 1 (1989).

[35] G. Audi, A.H. Wapstra, *Nucl. Phys.* **A595**, 409 (1995).

[36] P. Möller, J.R. Nix, W.D. Myers, W.J. Świątecki, *At. Data Nucl. Data Tables* **59**, 185 (1995).

[37] Electronic version of Nuclear Data Sheets, `http:www.dne.bnl.gov/nndc.html`

[38] Z. Łojewski, B. Nerlo-Pomorska, K. Pomorski, *Acta Phys. Pol.* **B25**, 1147 (1994).